JACS
JOURNAL OF THE AMERICAN CHEMICAL SOCIETY
pubs.acs.org/JACS
Article

An Ultrapotent and Selective Cyclic Peptide Inhibitor of Human β-Factor XIIa in a Cyclotide Scaffold

Wenyu Liu, Simon J. de Veer, Yen-Hua Huang, Toru Sengoku, Chikako Okada, Kazuhiro Ogata, Christina N. Zdenek, Bryan G. Fry, Joakim E. Swedberg, Toby Passioura,* David J. Craik,* and Hiroaki Suga*

Cite This: J. Am. Chem. Soc. 2021, 143, 18481−18489

ABSTRACT: Cyclotides are plant-derived peptides with complex structures shaped by their head-to-tail cyclic backbone and cystine knot core. These structural features underpin the native bioactivities of cyclotides, as well as their beneficial properties as pharmaceutical leads, including high proteolytic stability and cell permeability. However, their inherent structural complexity presents a challenge for cyclotide engineering, particularly for accessing libraries of sufficient chemical diversity to design potent and selective cyclotide variants. Here, we report a strategy using mRNA display enabling us to select potent cyclotide-based FXIIa inhibitors from a library comprising more than 10^{12} members based on the cyclotide scaffold of *Momordica cochinchinensis* trypsin inhibitor-II (MCoTI-II). The most potent and selective inhibitor, cMCoFx1, has a pM inhibitory constant toward FXIIa with greater than three orders of magnitude selectivity over related serine proteases, realizing specific inhibition of the intrinsic coagulation pathway. The cocrystal structure of cMCoFx1 and FXIIa revealed interactions at several positions across the contact interface that conveyed high affinity binding, highlighting that such cyclotides are attractive cystine knot scaffolds for therapeutic development.

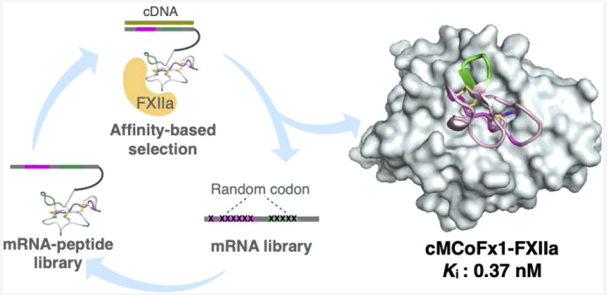

INTRODUCTION

Cyclotides are plant-derived head-to-tail cyclic peptides with a cystine knot topology (Figure 1a).[1] Their constrained cyclic and knotted structures provide them with exceptional thermal, chemical, and proteolytic stability compared with linear peptides,[2] and some cyclotides have been shown to be orally bioactive[3,4] and/or cell permeable.[5,6] Natural cyclotides display a wide range of host defense-related activities,[7] demonstrating their capability to exert potent biological effects. This combination of stability and potency, with the potential for oral activity, makes cyclotides appealing scaffolds for the development of next generation biologic therapies, agrichemical agents, or chemical probes.[8] In nature, the sequences of cyclotides have been progressively optimized for specific functions over millions of years of evolution. By contrast, the production of engineered cyclotides with new functions or altered target specificity requires similar levels of optimization but over a dramatically shorter time frame.

Despite extensive efforts, the generation of designer cyclotides with novel activity and specificity against pharmaceutical targets has proven to be challenging. One of the key obstacles is the complex nature of the cyclotide scaffold, with difficulties in high-throughput production of cyclotide libraries placing a limitation on their accessible sequence or chemical diversity. Over the past two decades, a variety of cyclotide engineering strategies have been reported,[9] the majority of which involve "grafting" peptide epitopes with known target-binding functionality into the loops of cyclotide scaffolds to generate variants with novel target tropism.[10−14] This approach has been applied for generating cyclotides with activities relevant to human diseases, including HIV,[10] cancer,[11,14] and pain.[3] However, such engineering has largely relied on pre-existing peptide epitopes that are not necessarily optimal for cyclotides, and the resulting molecules have consequently exhibited relatively moderate levels of activity, e.g. dissociation or inhibitory constants that generally fall in the micromolar or submicromolar range.

In another approach, several cyclotide-based protease inhibitors have been generated through rational approaches designed to bias the specificity of potent natural trypsin inhibitors (the *Momordica cochinchinensis* derived cyclotides, MCoTI-I and MCoTI-II) toward other serine protease targets.[15−18] One particularly appealing target in this respect

Received: July 21, 2021
Published: November 1, 2021

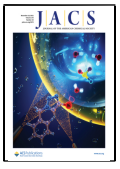

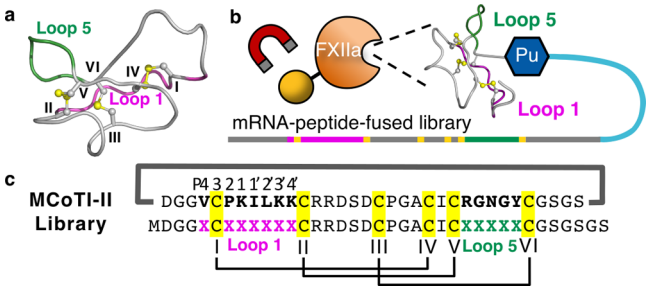

Figure 1. (a) Structure of the prototypic trypsin inhibitor cyclotide MCoTI-II (PDB 4GUX)[38] showing the head-to-tail cyclic backbone and knotted arrangement of three disulfide bonds deriving from six conserved Cys residues (labeled I–VI). Backbone regions between the Cys residues are referred to as loops. (b) Schematic illustration of the mRNA display strategy for discovery of FXIIa inhibitors based on the MCoTI-II scaffold whereby a single Val residue in loop 6, and all of loops 1 (colored magenta) and 5 (colored green) are varied (Pu = puromycin). (c) Sequence of native MCoTI-II showing the disulfide connectivity (black lines) and head-to-tail cyclic backbone (thick gray line). Key contact residues P4–P1 and P1′–P4′ sites (Schechter–Berger nomenclature) are indicated above the sequence. The lower sequence shows the regions of sequence varied in the display library (magenta and green residues).

is coagulation factor XIIa (FXIIa), a trypsin-like serine protease that initiates the intrinsic pathway of the coagulation system. Inhibition of FXIIa has been proposed as a strategy for developing safer therapies for thromboembolic and inflammatory diseases[19,20] based on the fact that, unlike most clotting factors, FXIIa deficiency is not associated with a bleeding disorder.[21,22] Previously, FXIIa inhibitors based on MCoTI-II were generated by screening a limited number of synthetic cyclotides bearing mutations in loop 1 (the primary binding loop of trypsin inhibitor cyclotides).[18] However, the potency of these molecules against FXIIa is ∼1000-fold lower than that shown by MCoTI-II against trypsin (K_i = 30 pM)[23] and they have poor selectivity. Other cyclotide-based inhibitors of disease-related serine proteases, including β-tryptase, neutrophil elastase, and matriptase, have also been reported,[15−17] and as for the FXIIa inhibitors, none have been sufficiently potent and selective to warrant further development.

Peptide display-based selection is an alternative approach to discover ligands for pharmaceutical targets from a library of sequence-diverse cyclotides. For example, *E. coli* and yeast surface display systems have been used to obtain cyclotide mutants against matriptase-1 and neuropilin-1 where the most active mutants have shown impressive activities (K_i = 0.83 nM to matriptase-1 using the MCoTI-II scaffold and K_D = 34 nM to neuropilin-1 using the kalata B1 scaffold).[24−26] Despite the remarkable inhibitory activity observed in the former case, the selectivity over trypsin (K_i = 36 nM) was limited to 40-fold. Although the theoretical diversities of the *E. coli* or yeast display systems could be up to 10^9 variants, it is difficult to accurately estimate the expression of correctly folded cyclotide variants in such cellular systems. In addition, the periplasmic disulfide formation or peptide folding may interfere with the cellular export efficiency.[24] This fact might have given a lower diversity than the theoretical value, yet resulting in nonoptimal cyclotide variants.

We envisioned that mRNA *in vitro* display, capable of affording substantially higher library diversities than other display techniques, may offer an improved route to identify cyclotides with high potency and selectivity against proteins of interest. This display system was previously applied on a backbone-acyclic knottin scaffold, *Ecballium elaterium* trypsin inhibitor-II (EETI-II), with *in vitro* translation achieved using the rabbit reticulocyte lysate system.[27] The library was screened against its natural target bovine trypsin, and the most potent binding sequence identified (K_D = 16 nM) was identical to wild type EETI-II, thus failing to produce improved *de novo* species. No other reports have emerged on this topic, and the use of mRNA display to evolve cystine knot peptides for new targets has not been demonstrated. One key question relates to the degree of sequence variation that is compatible with formation of the cystine knot, as randomizing multiple residues in the scaffold might prevent correct folding for certain non-native sequences. We hypothesized that an optimal *in vitro* translation system is needed to maintain high library diversity (and potentially compensate for folding losses) to enable selection of potent and selective variants.

Here we have applied mRNA display with a fully reconstituted *in vitro* translation system, referred to as FIT (Flexible *In-vitro* Translation) system,[28] for affinity-based selection of MCoTI-II analogues against human β-FXIIa (FXIIa, Figure 1b). We show that an acyclic analogue of MCoTI-II, equipped with an N-terminal formyl-M residue and a C-terminal dipeptide linker, is amenable to *in vitro* translation, allowing us to construct a highly diverse peptide library (Figure 1c). The selection afforded various FXIIa-binding variants, one of which, referred to as cMCoFx1, exhibited high FXIIa inhibitory potency (K_i = 0.37 nM), exquisite target selectivity over other related proteases (>3000-fold), high stability in human serum, and biological activity in coagulation assays. Further, X-ray analysis of cMCoFx1 and FXIIa cocrystals revealed the structural basis for potent and selective FXIIa inhibition.

RESULTS AND DISCUSSION

Affinity Selection of an MCoTI-II-Based Peptide Library against FXIIa. mRNA display requires the C-terminal fusion of peptides to their cognate mRNAs, generally making it challenging to display head-to-tail cyclic peptides.[29] Although the cystine knot scaffold of MCoTI-II bears a head-to-tail cyclized structure, it adopts its bioactive conformation with three disulfide bonds even when linearized by breaking the cyclic backbone in loop 6.[23] This property of MCoTI-II provides a means of fusing to cognate mRNA via the C-terminal region. Furthermore, several homologous acyclic cystine knot peptides exist in nature that have similar folds and inhibitory potency to trypsin-inhibiting cyclotides.[30,31] Thus, we designed a backbone-acyclic library containing semirandomized MCoTI-II analogues for mRNA display.

To assess the feasibility of such an approach, we first translated a peptide corresponding to a backbone-acyclic version of native MCoTI-II in our FIT system.[28] This sequence was designed such that the normally head-to-tail cyclic MCoTI-II scaffold was split between the S and D residues in loop 6, with an N-terminal formyl-M residue added for translation initiation and a G-S dipeptide embedded in the C-terminus as a spacer for linkage to the cognate mRNA template via puromycin (Figure S1a). LC-MS analysis demonstrated that this *in vitro* translated acyclic peptide adopted a single conformation with a similar retention time to synthetic (without *N*-formyl-M or C-terminal G-S dipeptide) backbone cyclic or acyclic (linearized as above through splitting the S-D peptide bond in loop 6) MCoTI-II, indicating

https://doi.org/10.1021/jacs.1c07574
J. Am. Chem. Soc. 2021, 143, 18481−18489

that the correct cystine knot topology could be achieved in this system (Figure S1a).

Encouraged by this finding, we next sought to construct and screen a MCoTI-II-based library to identify variants bearing potent binding activity against FXIIa. We generated a semirandomized peptide library based on the linearized and translatable MCoTI-II scaffold described above, such that the residues predicted to interact with trypsin-like proteases (all of loops 1 and 5, and a V residue in loop 6) were randomized to allow the occurrence of any of the 20 canonical amino acids at these 12 positions (Figure 1c). These positions included all eight residues flanking the scissile bond in MCoTI-II (the P4−P1 and P1′−P4′ sites), with the exception of the C residue at the P3 site, which was fixed to allow formation of the native cystine knot.

Following a standard selection protocol,[32,33] the DNA encoding this library was assembled from degenerate oligonucleotides (Table S1), transcribed into mRNA, ligated to a puromycin-linked oligonucleotide, and translated *in vitro* to produce a library of mRNA-peptide fusion molecules. Based on the maximum amount of ribosome in the *in vitro* translation cocktail, the theoretical diversity of the mRNA-peptide fusion library was more than 10^{14} variants. However, the diversity was likely decreased during mRNA display processes (e.g., mRNA library gel purification and puromycin ligation) or due to the possible formation of misfolded variants. Therefore, we conservatively estimated that the mRNA-peptide fusion library comprised in excess of 10^{12} variants.[34] This complexity of sequence space that can be explored by affinity selection is far larger than other approaches. The library was reverse transcribed and screened for affinity to biotinylated FXIIa immobilized on streptavidin-coated magnetic beads. After four rounds of selection (Figure S2), next-generation sequencing (NGS) was performed to identify clonal sequences within the enriched cDNA library after the third and fourth rounds (full sequencing data available via the DNA Data Bank of Japan Sequence Read Archive (DRA) with accession number DRA012755). The 19 most abundant sequences exhibited high clonal convergence, considering each sequence was enriched from a single clone in the original library.

Strikingly, the 19 most abundant sequences exhibited sequence homology to MCoTI-II near the scissile bond in loop 1 (Figure 2). Hydrophobic or basic residues were preferred at the P4 site, and the P residue at position 6 (P6) in the P2 site was highly conserved (identical to MCoTI-II). Moreover, substitutions with R (R7) and a hydrophobic residue (I/L/V8) at P1 and P1′ sites, respectively, were frequently observed in the selected sequences. Interestingly, it was previously shown that the K7R substitution favors binding to FXIIa, and endogenous FXIIa substrates and inhibitors including FXI, plasma kallikrein, serpin C1, and antithrombin also have an R residue at the P1 site.[35] The inherent preference for R7 at the P1 site by FXIIa is possibly due to the deeper S1 pocket in FXIIa relative to trypsin, which allows the longer side chain on R7 to form a direct ionic bond with Asp189 (chymotrypsin numbering) positioned at the base of the S1 pocket.

In contrast to the conservation observed for the P4, P2, P1, and P1′ sites, residues at the P2′−P4′ sites were less conserved, but some preference trends were observed (Figure 2). Whereas MCoTI-II has consecutive K10 and K11 at the P3′ and P4′ sites, respectively, the affinity-selected peptides had a combination of hydrophobic residues (V, L, F, W, or P) or a

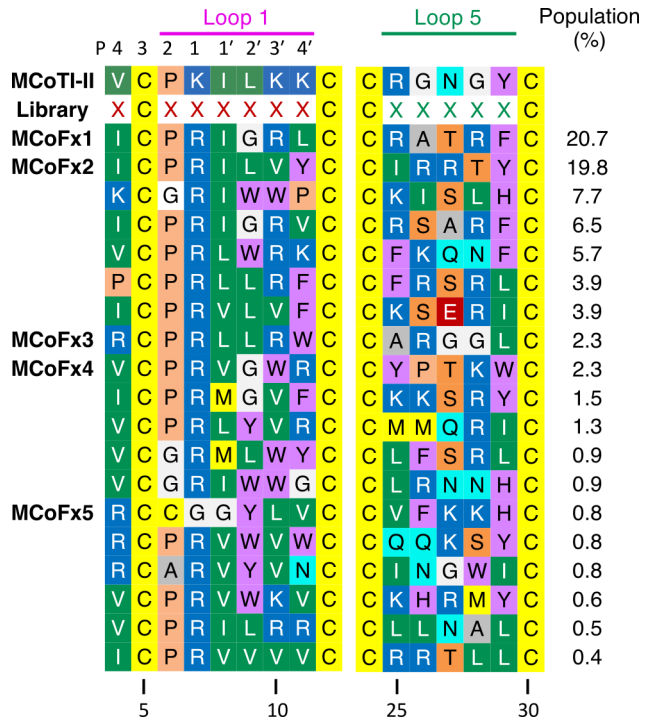

Figure 2. Sequences of the randomized region in the top 19 most abundant peptides recovered from affinity selection against FXIIa. The right column population (%) indicates the proportion of each sequence in the total recovered library. The sequence of MCoTI-II is shown above the selected peptides. The lower numbers indicate the position of the residues in the peptide.

combination of a hydrophobic residue and a basic residue (R or K). This trend suggests that strong electrostatic interactions at these sites are not crucial for FXIIa binding. Since both R and K residues also possess a long hydrocarbon chain with a basic headgroup, the aliphatic moiety on the side chain could additionally facilitate hydrophobic interactions with the FXIIa surface. In contrast to loop 1, alignment of the loop 5 sequences showed little conservation, although one or two R or K residues were generally observed (Figure 2). This suggests that the basic residues possibly contribute to an electrostatic interaction with FXIIa and/or the peptide itself to improve its structural rigidity. An unusual sequence, MCoFx5, contained an additional C6 and a G7 at P2 and P1 sites, replacing the conserved P6 and R7 residues, respectively. However, since we observed that MCoFx5 displayed a subtle loss of activity compared with MCoTI-II (*vide infra*), these mutations did not appear to be beneficial for FXIIa binding.

Selected FXIIa-binding peptides are potent FXIIa inhibitors. Five peptides (designated MCoFx1−5) from the top 19 selected sequences were chosen for solid-phase peptide synthesis (SPPS)[36] and characterization. Both backbone-acyclic (as selected during display screening) and cyclic forms of each sequence were synthesized to determine the effect of backbone cyclization on FXIIa binding and inhibitory activity. The synthetic peptides were purified by RP-HPLC and characterized by analytical HPLC (Figure S1b) and MALDI-TOF mass spectroscopy (Table S2). Conformations of each peptide were assessed by ^{1}H NMR spectroscopy, which showed comparable peak patterns to those of MCoTI-II (Figure S3a). Moreover, the α-proton NMR secondary chemical shifts of cMCoFx1 (Figure S3b) indicated that

https://doi.org/10.1021/jacs.1c07574
J. Am. Chem. Soc. 2021, 143, 18481−18489

Peptide	Loop 1 / Sequence / Loop 5	K_D (nM) Acyclic	K_D (nM) Cyclic	K_i (nM) Acyclic	K_i (nM) Cyclic
MCoTI-II	DGGVCPKILKKCRRDSDCPGACICRGNGYCGSGS		58 ± 8		129 ± 9
MCoFx1	DGGICPRIGRLCRRDSDCPGACICRATRFCGSGY	1.9 ± 0.04	0.90 ± 0.04	0.73 ± 0.2	0.37 ± 0.04
MCoFx2	DGGICPRILVYCRRDSDCPGACICIRRTYCGSGS	45 ± 3	10 ± 1	73 ± 3	12 ± 0.7
MCoFx3	DGGRCPRLLRWCRRDSDCPGACICARGGLCGSGS	167 ± 40	23 ± 2	525 ± 30	75 ± 3
MCoFx4	DGGVCPRVGWRCRRDSDCPGACICYPTKWCGSGS	74 ± 6	14 ± 1	17 ± 0.9	5.5 ± 0.5
MCoFx5	DGGRCCGGYLVCRRDSDCPGACICVFKKHCGSGS	23 ± 0.4	82 ± 3	106 ± 7	207 ± 9

Figure 3. FXIIa binding affinity (K_D) and inhibitory activity (K_i) of chemically synthesized MCoTI-II and acyclic or cyclic MCoFx1−5.

a

```
                  Loop 1                Loop 5
MCoTI-II    DGGVCPKILKKCRRDSDCPGACICRGNGYCGSGS
cMCoFx1     DGGICPRIGRLCRRDSDCPGACICRATRFCGSGY
cMCoTI-fxL1 DGGICPRIGRLCRRDSDCPGACICRGNGYCGSGS
cMCoTI-fxL5 DGGVCPKILKKCRRDSDCPGACICRATRFCGSGS
                5   10   15   20   25   30
```

b

	cMCoFx1	cMCoTI-fxL1	cMCoTI-fxL5
FXIIa	K_i = 0.37 ± 0.04 nM	K_i = 0.69 ± 0.04 nM	K_i = 66 ± 0.8 nM
Trypsin	K_i = 1110 ± 36 nM	K_i = 996 ± 17 nM	K_i = 0.08 ± 0.005 nM
FXa	IC_{50} > 5 μM (0%)	IC_{50} > 5 μM (0%)	IC_{50} > 5 μM (0%)
FXIa	IC_{50} > 5 μM (0%)	IC_{50} > 5 μM (1%)	IC_{50} > 5 μM (1%)
Thrombin	IC_{50} > 5 μM (2%)	IC_{50} > 5 μM (1%)	IC_{50} > 5 μM (3%)
Plasma kallikrein	IC_{50} > 5 μM (0%)	IC_{50} > 5 μM (0%)	IC_{50} > 5 μM (0%)
Plasmin	IC_{50} > 5 μM (13%)	IC_{50} > 5 μM (19%)	K_i = 31 ± 4 nM
uPA	IC_{50} > 5 μM (0%)	IC_{50} > 5 μM (0%)	IC_{50} > 5 μM (0%)
tPA	IC_{50} > 5 μM (0%)	IC_{50} > 5 μM (1%)	IC_{50} > 5 μM (1%)
Matriptase	K_i = 9120 ± 760 nM	K_i = 2210 ± 130 nM	K_i = 17 ± 0.8 nM

Figure 4. (a) Sequences of MCoTI-II, cMCoFx1 and two loop-grafted variants, cMCoTI-fxL1 and cMCoTI-fxL5, where loop 1 or loop 5 in MCoTI-II was replaced by the optimized sequence in cMCoFx1. (b) Inhibitory activity of cMCoFx1, cMCoTI-fxL1, and cMCoTI-fxL5 against a panel of serine proteases. K_i was determined for inhibitors with IC_{50} < 5 μM against a given protease. The percentage value in brackets indicates percent inhibition at 5 μM for the off-target proteases.

cMCoFx1 adopted the native-like conformation of MCoTI-II. Some differences in chemical shifts were observed in loops 1 and 5, corresponding to sequence divergence from MCoTI-II.

Surface plasmon resonance (SPR) experiments demonstrated that all synthetic peptides exhibited FXIIa binding affinities in the nanomolar to picomolar range, regardless of backbone cyclization (Figure 3). cMCoFx1 exhibited the highest binding affinity, with a K_D of 900 pM, i.e. 60-fold higher affinity than MCoTI-II. Moreover, *in vitro* inhibition assays revealed that cMCoFx1 was the most active with a K_i of 370 pM, which is 350-fold more potent than MCoTI-II. To the best of our knowledge, this molecule is among the most potent FXIIa inhibitors reported to date. In general, the backbone cyclic analogues of each molecule (except MCoFx5) displayed 2−7-fold higher binding affinity and inhibitory activity (i.e., lower K_D and K_i values) than their acyclic forms, indicating that our screening strategy was not biased toward backbone acyclic analogues. The only exception was cMCoFx5, which displayed a slight loss of activity compared with aMCoFx5. However, as described above, the sequence of MCoFx5 differs substantially from MCoFx1−4, and it has lower activity against FXIIa than MCoTI-II.

MCoTI-II was originally identified as a potent trypsin inhibitor (K_i = 30 pM),[23] and consistent with this, SPR measurements in our study showed a K_D of less than 100 pM for synthetic MCoTI-II toward bovine trypsin (Table S3). Although FXIIa has 36% and 37% identity to human and bovine trypsin, respectively, the residues in the S1 pocket have far higher homology (~90%). Thus, we verified how selective our *de novo* FXIIa-inhibiting MCoTI-II analogues would be with respect to trypsin as an example of a related serine protease. We determined K_D values of cMCoFx1−5, as well as aMCoFx1−5, to examine their selectivity by SPR. The most potent FXIIa inhibitor, cMCoFx1, exhibited 60-fold greater affinity for FXIIa and 300-fold lower affinity for trypsin compared with K_D values of MCoTI-II (Table S3). Interestingly, cMCoFx2 showed improved binding to FXIIa (K_D = 10 nM) compared with MCoTI-II (K_D = 58 nM), yet its binding affinity also remained high to trypsin (K_D less than 100 pM). Because cMCoFx1 and cMCoFx2 are identical at the P4, P2, P1, and P1′ sites, the selectivity of cMCoFx1 for FXIIa

https://doi.org/10.1021/jacs.1c07574
J. Am. Chem. Soc. 2021, 143, 18481−18489

over trypsin must arise from differences between these two molecules at the P2′−P4′ sites and/or in loop 5. A similar trend was observed for cMCoFx3 and cMCoFx4, which exhibit 2−3-fold improved affinity for FXIIa compared to MCoTI-II, but nonetheless have 2−8-fold higher affinity for trypsin.

Neither aMCoFx5 nor cMCoFx5 showed detectable affinity for trypsin (Table S3). As discussed earlier, the loop 1 sequence of these peptides diverges substantially from the other FXIIa inhibitors identified. Although the origin of this high selectivity is not clear, we speculate that the unique C6 mutation at P2 site as well as consecutive G7 and G8 mutations at P1 and P1′ sites may alter the entire loop, resulting in presentation of a different loop structure or possibly altered folding compared with MCoTI-II. Such an unexpected structural change could eliminate the original interaction with trypsin occurring via loop 1, and instead create a new interface between MCoFx5 and FXIIa, leading to the observed highly selective interaction even though the inhibitory activity is relatively moderate (K_i = 106 nM, Figure 3).

In addition to trypsin, we examined the binding affinity of the selected peptides toward factor XII (FXII), the zymogen form of FXIIa. SPR measurements revealed that none of the selected peptides exhibited a FXII-binding response at a concentration of 5 μM (Figure S4). The X-ray crystal structure of the FXII protease domain reveals that several key binding pockets are not properly formed in the zymogen, including the S1 pocket and oxyanion hole,[37] which may explain the weak binding of active site targeted peptides, such as MCoTI-II analogues.

cMCoFx1 variants selectively inhibit FXIIa and the intrinsic coagulation pathway. To further characterize the inhibitory activity of cMCoFx1, we synthesized two chimeric peptides, referred to as cMCoTI-fxL1 and cMCoTI-fxL5, where the peptide motif from either loop 1 or loop 5 of cMCoFx1 was grafted into the respective loop of MCoTI-II (Figure 4a). A comparison of the α-proton NMR chemical shifts of cMCoTI-fxL1 and cMCoTI-fxL5 (Figure S3b) showed they were similar to their parent peptides in their respective regions. For instance, the secondary Hα shifts for loop 1 of cMCoTI-fxL1 were similar to those of cMCoFx1, whereas loop 1 of cMCoTI-fxL5 was comparable to MCoTI-II.

We next expanded the activity screen for cMCoFx1 and the single loop-grafted variants from FXIIa to other clinically relevant serine proteases (Figure 4b). These assays revealed that the difference in K_i for cMCoFx1 against FXIIa (0.37 nM) and trypsin (1110 nM) exceeds three orders of magnitude. Remarkably, cMCoFx1 shows almost no inhibitory activity against other serine proteases, confirming that cMCoFx1 is highly specific for FXIIa. cMCoTI-fxL1 exhibits a similar profile to cMCoFx1, although its potency against FXIIa (K_i = 0.69 nM) and selectivity with respect to trypsin and matriptase (K_i values of 996 and 2210 nM, respectively) are slightly lower. By contrast, cMCoTI-fxL5 displays nearly the same potency and selectivity as MCoTI-II; i.e., K_i values for FXIIa, trypsin, and matriptase are 66, 0.08, and 17 nM, respectively. These results clearly demonstrate that the sequence of loop 1 plays a major role in determining the potency and selectivity of MCoTI-II analogues, although the sequence of loop 5 does provide a subtle enhancement to the overall activity of cMCoFx1.

Having identified two potent and selective FXIIa inhibitors (cMCoFx1 and cMCoTI-fxL1), we next performed coagulation assays to assess their biological activity in human plasma. Inhibition of FXIIa was examined in activated partial thromboplastin time (aPTT) assays, where addition of kaolin initiates the intrinsic pathway via activation of FXII. Both inhibitors prolonged the clotting time in a dose-dependent manner and maintained substantial activity in the nanomolar range (Figure 5), as seen by the concentration of inhibitor required to double the clotting time observed in control assays ($EC_{2\times}$). By this measure, cMCoTI-fxL1 was slightly more potent than cMCoFx1 ($EC_{2\times}$ = 500 nM vs 702 nM), although this subtle difference between the two inhibitors could be due to variation in the experimental conditions between coagulation assays and prior enzyme kinetic assays.

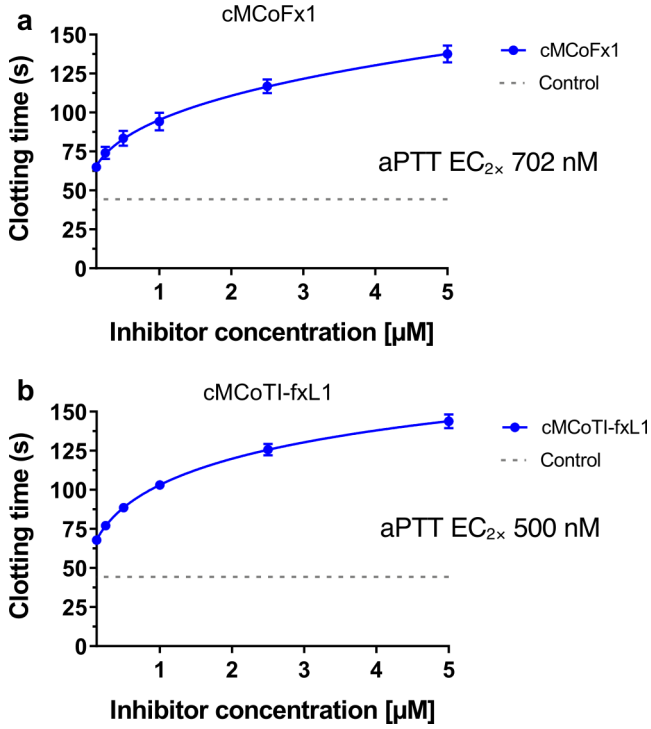

Figure 5. Inhibitory activity of (a) cMCoFx1 and (b) cMCoTI-fxL1 in activated partial thromboplastin time (aPTT) assays that measure clotting via the intrinsic pathway. The concentration of inhibitor required to double the clotting time observed in control assays (44.3 s, gray dashed line, buffer replaces addition of inhibitor) is shown as $EC_{2\times}$. Data points represent the mean ± standard deviation (n = 3).

We also performed prothrombin time (PT) assays to confirm that both inhibitors are selective for the intrinsic pathway (Figure S5). No significant differences in clotting time compared to control assays were observed for cMCoFx1 and cMCoTI-fxL1 at 10 μM, demonstrating that the potent and selective activity of these inhibitors identified in biochemical assays extends to biological assays in human plasma.

Structure of the cMCoFx1-FXIIa Complex. To understand the structural basis of the specific interaction between cMCoFx1 and FXIIa, we determined the cocrystal structure of their complex at 2.0 Å resolution (Figure 6a, PDB 7FBP). As expected, cMCoFx1 adopts a highly similar overall conformation to MCoTI-II[38] with a cystine knot topology (Figure 6b, PDB 4GUX, root-mean-square deviation of 0.47 Å for the 34 Cα atoms). The interaction mode is also similar between the cMCoFx1-FXIIa complex and the MCoTI-II-trypsin complex. R7 at the P1 site of cMCoFx1 (corresponding to K7 of MCoTI-II) inserts into the S1 pocket of FXIIa, making

https://doi.org/10.1021/jacs.1c07574
J. Am. Chem. Soc. 2021, 143, 18481−18489

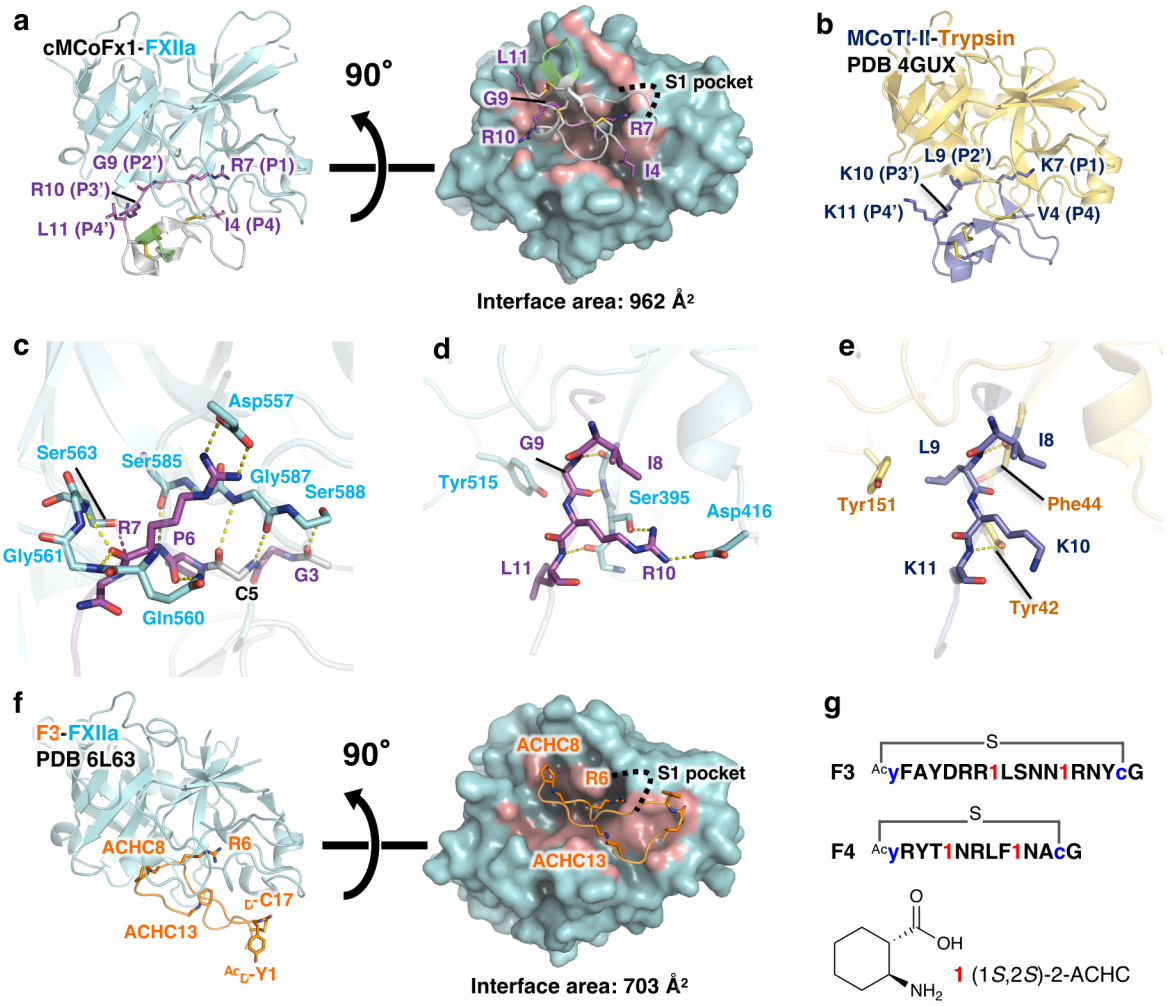

Figure 6. Structural analysis of the cMCoFx1-FXIIa complex. (a) Left: The cartoon model of the overall structure of cMCoFx1 (gray, with residues I4, P6-L11 highlighted in magenta and R25-F29 highlighted in green) bound with FXIIa (cyan) (PDB 7FBP). The loop 1 residues on cMCoFx1 that differ from MCoTI-II (I4, R7, G9, R10, and L11) and six C residues are shown as a stick model. Right: interaction surface. cMCoFx1 and FXIIa are shown as cartoon and surface models, respectively. The FXIIa atoms within 3.9 Å from any cMCoFx1 atoms are colored red. (b) Overall structure of MCoTI-II (slate) bound with trypsin (yellow) (PDB 4GUX). The corresponding loop 1 residues on MCoTI-II that differ from cMCoFx1 (V4, K7, L9, K10, and K11) and six C residues are shown as a stick model. (c) Interactions between cMCoFx1 and FXIIa near cMCoFx1 R7. (d) Interactions between cMCoFx1 and FXIIa near cMCoFx1 G9 and R10. (e) Interactions between MCoTI-II and trypsin near MCoTI-II L9 and K10. (f) Structure of the F3-FXIIa complex (PDB 6L63). Left: The cartoon model of the overall structure of F3 (orange) bound with FXIIa (cyan). R6, two ACHC residues, and the residues mediating macrocyclization ($^{Ac}{}_{D}$-Y1 and $_{D}$-C17) of F3 are shown as a stick model. Right: interaction surface. F3 and FXIIa are shown as cartoon and surface models, respectively. The FXIIa atoms within 3.9 Å from any F3 atoms are colored red. (g) Peptide sequences of cbAA-containing F3 and F4. Red sequence number: 1, (1*S*,2*S*)-2-ACHC. Blue sequence: D-amino acids. The peptides are macrocyclized with a thioether bond which was formed between ^{Ac}D-Y1 and D-C17 or D-C13, respectively.

an ionic interaction and two hydrogen bonds with Asp557 of FXIIa (Figure 6a,c).

cMCoFx1 forms intermolecular β-sheet-like hydrogen bonds with FXIIa at two regions (residues C5−P6 and G9−L11 in Figure 6c,d). Moreover, the R7 carbonyl oxygen at the P1 site forms two hydrogen bonds with the mainchain nitrogen atoms of Gly561 and Ser563 of FXIIa, and the R7 carbonyl carbon is located 2.8 Å away from the catalytic Ser563 side chain, suitable for nucleophilic attack (Figure 6c). The P6 carbonyl oxygen forms a hydrogen bond with the side chain of FXIIa Gln560 (Figure 6c). These interactions are similar to those seen in the MCoTI-II-trypsin complex.

Our functional analysis of cMCoTI-fxL1/L5 suggested that residues in loop 1 are primarily responsible for the high potency and selectivity of cMCoFx1. The X-ray structure suggested that G9 and R10 of cMCoFx1 (corresponding to L9 and K10 of MCoTI-II, respectively) are the key determinants. G9 is located close to the side chain of FXIIa Tyr515, and substituting G9 with a larger residue would cause a steric clash with Tyr515 (Figure 6d). In the MCoTI-II-trypsin complex, the corresponding Tyr residue (Tyr151) adopts a different conformation, making hydrophobic interaction with L9 of MCoTI-II (Figure 6e). R10 of cMCoFx1 forms hydrogen bonds with Ser395 and Asp416, but no such interactions are formed by K10 in the MCoTI-II-trypsin complex (Figure 6d,e).

We recently reported a FXIIa-inhibiting monomacrocyclic peptide, F3 (K_i = 1.5 nM), containing cyclic β-amino acids (cbAAs) and its cocrystal structure with FXIIa (Figure 6f,g).[39] Two cbAAs were incorporated in F3, inducing γ-turns that stabilize the compact antiparallel β-sheet structure. In the case of cMCoFx1, the rigid conformation of the peptide is stabilized

https://doi.org/10.1021/jacs.1c07574
J. Am. Chem. Soc. 2021, 143, 18481−18489

by the cystine knot. Structural comparison revealed that both F3 and cMCoFx1 bind to the active site of FXIIa in a similar manner, where the R side chain (R7 in cMCoFx1 or R6 in F3) was deeply inserted into the S1 pocket (Figure 6a,f). cMCoFx1 shows a slightly larger interaction area than F3 (962 Å^2 vs 703 Å^2 in F3), which is consistent with its lower K_D and K_i values, i.e. higher potency. The separate discoveries of F3 and cMCoFx1 demonstrate that the technique of mRNA display is broadly applicable to *de novo* discovery of not only macrocyclic peptides containing nonproteinogenic amino acids (using the Random nonstandard Peptide Integrated Discovery, abbreviated as RaPID)[40] but also nature-inspired cystine-knot peptides.

Stability of cMCoFx1 Variants in Human Serum. We next evaluated the stability of aMCoFx1, cMCoFx1, and cMCoTI-fxL1 compared to MCoTI-II in human serum for up to 24 h at 37 °C (Figure S6a). All tested peptides showed high serum stability with half-lives of more than 24 h. A linear control peptide (EAIYAAPFAKKK) rapidly degraded in serum within 1 h. To verify the level of proteolytic activity in serum over the course of the above assay, we added the control peptide to serum at the time points of 4 and 24 h, which gave the same degradation profile as 1 h (Figure S6b), indicating that the serum proteases retained activity. The results clearly showed that aMCoFx1, cMCoFx1, and cMCoTI-fxL1 are highly resistant to serum proteases, similar to MCoTI-II.

Having shown that cMCoFx1 is stable in human serum, we assessed any potential cytotoxic effects of MCoTI-II and cMCoFx1 in cultured human umbilical vein endothelial cells (HUVECs). No cytotoxicity was observed after 24 h exposure to MCoTI-II or cMCoFx1 at concentrations up to 64 μM (Figure S7a). Additionally, as MCoTI-II has been reported to internalize into cells, experiments were performed to assess the cellular uptake of cMCoFx1 compared to MCoTI-II and the cell-penetrating peptide TAT. Peptides were fluorescently labeled to allow evaluation of peptide internalization into HUVECs using flow cytometry (Figure S7b). The results showed that cMCoFx1 has comparable cellular uptake efficiency to MCoTI-II but internalizes less efficiently than the established cell-penetrating peptide TAT.

As mentioned above, we recently developed two nonstandard cbAA-containing monomacrocyclic FXIIa inhibitors, F3 and F4 (Figure 6g), by means of the RaPID system.[39] Strikingly, cMCoFx1 exhibits approximately 5-fold and 26-fold higher inhibitory activity than F3 and F4, respectively. The half-life ($t_{1/2}$) of cMCoFx1 is about 24 h (or up to 40 h determined by an extrapolation of Figure S6a), while that of the nonstandard macrocycle F3 is about 60 h. The more compact macrocycle F4 exhibited even higher serum stability with $t_{1/2}$ over 285 h (>12 days). The greater proteolytic stability observed for F3 and F4 can be attributed to the existence of the unique β- and D-amino acids as well as the structurally compact monocyclic scaffold. It should be emphasized that cMCoFx1 also has a remarkable serum stability even though it comprises only proteinogenic amino acids. Clearly, the compact cystine knot structure of cMCoFx1 significantly contributes to the proteolytic resistance, yet the solvent exposed loops could leave the unwanted protease accessibility. We envision that the proteolytic stability of cMCoFx1 can be improved by either semirational mutations or a saturation mutagenesis display.[41]

Heinis et al. have also reported a series of phage display-based selection campaigns using thioether-linked bicyclic peptide libraries and devised a potent FXIIa inhibitor, referred to as FXII900, displaying an impressive potency similar to that of cMCoFx1 (K_i = 370 pM) and stability ($t_{1/2}$ more than 5 days in plasma).[42−44] Interestingly, the great stability of FXII900 is mainly due to the incorporation of noncanonical amino acids, similar to F3 and F4. Even though cMCoFx1 consists of only proteinogenic amino acids, it has yet a remarkable proteolytic stability, indicating that the cystine knot topology imparts such a property.

Collectively, the different display screens have generated a range of potent FXIIa-inhibiting molecules with unique structures, including the monocyclic F3/F4 peptides containing cbAAs, bicyclic FXII900, and the cystine knot cMCoFx1 molecule described in this study. Remarkably, despite targeting the same enzyme, the primary binding loop from each inhibitor type shows considerable sequence divergence, with P1 R as the only common residue. It should be noted that separate mRNA display screens have yielded potent monomacrocycle or cystine knot peptides from a single selection campaign, indicating its robustness and versatile applicability to various peptide scaffolds.

CONCLUSIONS

In this study, we used mRNA display with the FIT system for the discovery of potent FXIIa inhibitors from a cyclotide-based library containing two randomized loops. The most potent cyclotide analogue, cMCoFx1, inhibits FXIIa with a K_i of 370 pM, shows selectivity of more than three orders of magnitude over most other serine proteases, and potently inhibits coagulation via the intrinsic pathway in human plasma. Analysis of a cocrystal structure of cMCoFx1-FXIIa revealed substrate-like tight binding, with interactions between loop 1 of cMCoFx1 and FXIIa providing the largest contribution to the inhibitor's high potency and exquisite specificity. The structural stability preinstalled in the cyclotide scaffold has benefited the generation of not only potent but also proteolytically stable FXIIa inhibitors. Most interestingly, cMCoFx1 exhibits an inhibitory potency that approaches the level of MCoTI-II for trypsin, a product of evolution over millions of years, highlighting the immense potential of mRNA display as a method for rapidly evolving potent cyclotide variants with potential pharmaceutical value.

ASSOCIATED CONTENT

Supporting Information

The Supporting Information is available free of charge at https://pubs.acs.org/doi/10.1021/jacs.1c07574.

Additional figures, tables and experimental methods (PDF)

AUTHOR INFORMATION

Corresponding Authors

Hiroaki Suga − *Department of Chemistry, Graduate School of Science, The University of Tokyo, Tokyo 113-0033, Japan; Australian Research Council Centre of Excellence for Innovations in Peptide and Protein Science, Brisbane QLD 4072, Australia;* orcid.org/0000-0002-5298-9186; Email: hsuga@chem.s.u-tokyo.ac.jp

David J. Craik − *Australian Research Council Centre of Excellence for Innovations in Peptide and Protein Science, Brisbane QLD 4072, Australia; Institute for Molecular Bioscience, The University of Queensland, Brisbane, QLD*

4072, Australia; orcid.org/0000-0003-0007-6796; Email: d.craik@imb.uq.edu.au

Toby Passioura − *Department of Chemistry, Graduate School of Science, The University of Tokyo, Tokyo 113-0033, Japan; Australian Research Council Centre of Excellence for Innovations in Peptide and Protein Science, Brisbane QLD 4072, Australia; School of Life and Environmental Sciences, School of Chemistry and Sydney Analytical, The University of Sydney, Sydney, NSW 2006, Australia;* orcid.org/0000-0002-6089-5067; Email: toby.passioura@sydney.edu.au

Authors

Wenyu Liu − *Department of Chemistry, Graduate School of Science, The University of Tokyo, Tokyo 113-0033, Japan*

Simon J. de Veer − *Australian Research Council Centre of Excellence for Innovations in Peptide and Protein Science, Brisbane QLD 4072, Australia; Institute for Molecular Bioscience, The University of Queensland, Brisbane, QLD 4072, Australia;* orcid.org/0000-0002-7041-9937

Yen-Hua Huang − *Australian Research Council Centre of Excellence for Innovations in Peptide and Protein Science, Brisbane QLD 4072, Australia; Institute for Molecular Bioscience, The University of Queensland, Brisbane, QLD 4072, Australia;* orcid.org/0000-0001-6937-2660

Toru Sengoku − *Department of Biochemistry, Graduate School of Medicine, Yokohama City University, Yokohama, Kanagawa 236-0004, Japan*

Chikako Okada − *Department of Biochemistry, Graduate School of Medicine, Yokohama City University, Yokohama, Kanagawa 236-0004, Japan*

Kazuhiro Ogata − *Department of Biochemistry, Graduate School of Medicine, Yokohama City University, Yokohama, Kanagawa 236-0004, Japan*

Christina N. Zdenek − *Venom Evolution Lab, School of Biological Sciences, The University of Queensland, Brisbane, QLD 4072, Australia*

Bryan G. Fry − *Venom Evolution Lab, School of Biological Sciences, The University of Queensland, Brisbane, QLD 4072, Australia*

Joakim E. Swedberg − *Institute for Molecular Bioscience, The University of Queensland, Brisbane, QLD 4072, Australia*

Complete contact information is available at: https://pubs.acs.org/10.1021/jacs.1c07574

Notes

The authors declare the following competing financial interest(s): H.S. and D.C. have filed a patent application on the molecules reported in this article with the Australian Provisional Patent Application Number 2021903307.

■ ACKNOWLEDGMENTS

This work was supported by a Japan Society for the Promotion of Sciences (JSPS) Grant-in-Aid for JSPS fellows (20J11284) to W.L.; the patent royalty foundation to H.S.; Platform Project for Supporting Drug Discovery and Life Science Research (Basis for Supporting Innovative Drug Discovery and Life Science Research) from Japan Agency for Medical Research and Development (AMED) under Grant Number JP19am0101070 (support number 1698); National Health and Medical Research Council (NHMRC) Grants GNT1164412 and GNT1120066; and Australian Research Council (ARC) grant CE200100012 to D.C.

■ REFERENCES

(1) Craik, D. J.; Daly, N. L.; Bond, T.; Waine, C. Plant cyclotides: a unique family of cyclic and knotted proteins that defines the cyclic cystine knot structural motif. *J. Mol. Biol.* **1999**, *294* (5), 1327−1336.

(2) Colgrave, M. L.; Craik, D. J. Thermal, chemical, and enzymatic stability of the cyclotide kalata B1: the importance of the cyclic cystine knot. *Biochemistry* **2004**, *43* (20), 5965−5975.

(3) Wong, C. T.; Rowlands, D. K.; Wong, C. H.; Lo, T. W.; Nguyen, G. K.; Li, H. Y.; Tam, J. P. Orally active peptidic bradykinin B1 receptor antagonists engineered from a cyclotide scaffold for inflammatory pain treatment. *Angew. Chem., Int. Ed.* **2012**, *51* (23), 5620−5624.

(4) Thell, K.; Hellinger, R.; Sahin, E.; Michenthaler, P.; Gold-Binder, M.; Haider, T.; Kuttke, M.; Liutkeviciute, Z.; Goransson, U.; Grundemann, C.; Schabbauer, G.; Gruber, C. W. Oral activity of a nature-derived cyclic peptide for the treatment of multiple sclerosis. *Proc. Natl. Acad. Sci. U. S. A.* **2016**, *113* (15), 3960−3965.

(5) Cascales, L.; Henriques, S. T.; Kerr, M. C.; Huang, Y. H.; Sweet, M. J.; Daly, N. L.; Craik, D. J. Identification and characterization of a new family of cell-penetrating peptides: cyclic cell-penetrating peptides. *J. Biol. Chem.* **2011**, *286* (42), 36932−36943.

(6) Henriques, S. T.; Huang, Y. H.; Chaousis, S.; Sani, M. A.; Poth, A. G.; Separovic, F.; Craik, D. J. The prototypic cyclotide kalata B1 has a unique mechanism of entering cells. *Chem. Biol.* **2015**, *22* (8), 1087−1097.

(7) Huang, Y. H.; Du, Q.; Craik, D. J. Cyclotides: Disulfide-rich peptide toxins in plants. *Toxicon* **2019**, *172*, 33−44.

(8) Wang, C. K.; Craik, D. J. Designing macrocyclic disulfide-rich peptides for biotechnological applications. *Nat. Chem. Biol.* **2018**, *14* (5), 417−427.

(9) de Veer, S. J.; Weidmann, J.; Craik, D. J. Cyclotides as tools in chemical biology. *Acc. Chem. Res.* **2017**, *50* (7), 1557−1565.

(10) Aboye, T. L.; Ha, H.; Majumder, S.; Christ, F.; Debyser, Z.; Shekhtman, A.; Neamati, N.; Camarero, J. A. Design of a novel cyclotide-based CXCR4 antagonist with anti-human immunodeficiency virus (HIV)-1 activity. *J. Med. Chem.* **2012**, *55* (23), 10729−10734.

(11) Ji, Y.; Majumder, S.; Millard, M.; Borra, R.; Bi, T.; Elnagar, A. Y.; Neamati, N.; Shekhtman, A.; Camarero, J. A. In vivo activation of the p53 tumor suppressor pathway by an engineered cyclotide. *J. Am. Chem. Soc.* **2013**, *135* (31), 11623−11633.

(12) Wang, C. K.; Gruber, C. W.; Cemazar, M.; Siatskas, C.; Tagore, P.; Payne, N.; Sun, G.; Wang, S.; Bernard, C. C.; Craik, D. J. Molecular grafting onto a stable framework yields novel cyclic peptides for the treatment of multiple sclerosis. *ACS Chem. Biol.* **2014**, *9* (1), 156−163.

(13) Chan, L. Y.; Craik, D. J.; Daly, N. L. Cyclic thrombospondin-1 mimetics: grafting of a thrombospondin sequence into circular disulfide-rich frameworks to inhibit endothelial cell migration. *Biosci. Rep.* **2015**, *35* (6), e00207.

(14) Huang, Y. H.; Henriques, S. T.; Wang, C. K.; Thorstholm, L.; Daly, N. L.; Kaas, Q.; Craik, D. J. Design of substrate-based BCR-ABL kinase inhibitors using the cyclotide scaffold. *Sci. Rep.* **2015**, *5*, 12974.

(15) Thongyoo, P.; Bonomelli, C.; Leatherbarrow, R. J.; Tate, E. W. Potent inhibitors of beta-tryptase and human leukocyte elastase based on the MCoTI-II scaffold. *J. Med. Chem.* **2009**, *52* (20), 6197−6200.

(16) Sommerhoff, C. P.; Avrutina, O.; Schmoldt, H. U.; Gabrijelcic-Geiger, D.; Diederichsen, U.; Kolmar, H. Engineered cystine knot miniproteins as potent inhibitors of human mast cell tryptase beta. *J. Mol. Biol.* **2010**, *395* (1), 167−175.

(17) Quimbar, P.; Malik, U.; Sommerhoff, C. P.; Kaas, Q.; Chan, L. Y.; Huang, Y. H.; Grundhuber, M.; Dunse, K.; Craik, D. J.; Anderson, M. A.; Daly, N. L. High-affinity cyclic peptide matriptase inhibitors. *J. Biol. Chem.* **2013**, *288* (19), 13885−13896.

(18) Swedberg, J. E.; Mahatmanto, T.; Abdul Ghani, H.; de Veer, S. J.; Schroeder, C. I.; Harris, J. M.; Craik, D. J. Substrate-guided design of selective FXIIa inhibitors based on the plant-derived *Momordica cochinchinensis* trypsin inhibitor-II (MCoTI-II) scaffold. *J. Med. Chem.* **2016**, *59* (15), 7287−7292.

(19) Renne, T.; Pozgajova, M.; Gruner, S.; Schuh, K.; Pauer, H. U.; Burfeind, P.; Gailani, D.; Nieswandt, B. Defective thrombus formation in mice lacking coagulation factor XII. *J. Exp. Med.* **2005**, *202* (2), 271−281.
(20) Nickel, K. F.; Long, A. T.; Fuchs, T. A.; Butler, L. M.; Renne, T. Factor XII as a therapeutic target in thromboembolic and inflammatory diseases. *Arterioscler., Thromb., Vasc. Biol.* **2017**, *37* (1), 13−20.
(21) Pauer, H. U.; Renne, T.; Hemmerlein, B.; Legler, T.; Fritzlar, S.; Adham, I.; Muller-Esterl, W.; Emons, G.; Sancken, U.; Engel, W.; Burfeind, P. Targeted deletion of murine coagulation factor XII gene-a model for contact phase activation *in vivo*. *Thromb. Haemostasis* **2004**, *92* (3), 503−508.
(22) Maas, C.; Renné, T. Coagulation factor XII in thrombosis and inflammation. *Blood* **2018**, *131* (17), 1903−1909.
(23) Avrutina, O.; Schmoldt, H. U.; Gabrijelcic-Geiger, D.; Le Nguyen, D.; Sommerhoff, C. P.; Diederichsen, U.; Kolmar, H. Trypsin inhibition by macrocyclic and open-chain variants of the squash inhibitor MCoTI-II. *Biol. Chem.* **2005**, *386* (12), 1301−1306.
(24) Getz, J. A.; Rice, J. J.; Daugherty, P. S. Protease-resistant peptide ligands from a knottin scaffold library. *ACS Chem. Biol.* **2011**, *6* (8), 837−844.
(25) Getz, J. A.; Cheneval, O.; Craik, D. J.; Daugherty, P. S. Design of a cyclotide antagonist of neuropilin-1 and −2 that potently inhibits endothelial cell migration. *ACS Chem. Biol.* **2013**, *8* (6), 1147−1154.
(26) Glotzbach, B.; Reinwarth, M.; Weber, N.; Fabritz, S.; Tomaszowski, M.; Fittler, H.; Christmann, A.; Avrutina, O.; Kolmar, H. Combinatorial optimization of cystine-knot peptides towards high-affinity inhibitors of human matriptase-1. *PLoS One* **2013**, *8* (10), e76956.
(27) Baggio, R.; Burgstaller, P.; Hale, S. P.; Putney, A. R.; Lane, M.; Lipovsek, D.; Wright, M. C.; Roberts, R. W.; Liu, R.; Szostak, J. W.; Wagner, R. W. Identification of epitope-like consensus motifs using mRNA display. *J. Mol. Recognit.* **2002**, *15* (3), 126−134.
(28) Goto, Y.; Katoh, T.; Suga, H. Flexizymes for genetic code reprogramming. *Nat. Protoc.* **2011**, *6* (6), 779−790.
(29) Takatsuji, R.; Shinbara, K.; Katoh, T.; Goto, Y.; Passioura, T.; Yajima, R.; Komatsu, Y.; Suga, H. Ribosomal synthesis of backbone-cyclic peptides compatible with in vitro display. *J. Am. Chem. Soc.* **2019**, *141* (6), 2279−2287.
(30) Hara, S.; Makino, J.; Ikenaka, T. Amino acid sequences and disulfide bridges of serine proteinase inhibitors from bitter gourd (*Momordica charantia* LINN.) seeds. *J. Biochem.* **1989**, *105* (1), 88−92.
(31) Le Nguyen, D.; Heitz, A.; Chiche, L.; Castro, B.; Boigegrain, R.; Favel, A.; Coletti-Previero, M. Molecular recognition between serine proteases and new bioactive microproteins with a knotted structure. *Biochimie* **1990**, *72*, 431−435.
(32) Hipolito, C. J.; Tanaka, Y.; Katoh, T.; Nureki, O.; Suga, H. A macrocyclic peptide that serves as a cocrystallization ligand and inhibits the function of a MATE family transporter. *Molecules* **2013**, *18* (9), 10514−10530.
(33) Katoh, T.; Goto, Y.; Suga, H. *In vitro selection of thioether-closed macrocycle peptide ligands by means of the RaPID system. Peptide Macrocycles: Methods and Protocols, Vol. 2371*; Springer: New York, NY, 2021.
(34) Yamagishi, Y.; Shoji, I.; Miyagawa, S.; Kawakami, T.; Katoh, T.; Goto, Y.; Suga, H. Natural product-like macrocyclic N-methyl-peptide inhibitors against a ubiquitin ligase uncovered from a ribosome-expressed de novo library. *Chem. Biol.* **2011**, *18* (12), 1562−1570.
(35) Gosalia, D. N.; Salisbury, C. M.; Ellman, J. A.; Diamond, S. L. High throughput substrate specificity profiling of serine and cysteine proteases using solution-phase fluorogenic peptide microarrays. *Mol. Cell. Proteomics* **2005**, *4* (5), 626−636.
(36) Cheneval, O.; Schroeder, C. I.; Durek, T.; Walsh, P.; Huang, Y. H.; Liras, S.; Price, D. A.; Craik, D. J. Fmoc-based synthesis of disulfide-rich cyclic peptides. *J. Org. Chem.* **2014**, *79* (12), 5538−5544.
(37) Pathak, M.; Wilmann, P.; Awford, J.; Li, C.; Hamad, B. K.; Fischer, P. M.; Dreveny, I.; Dekker, L. V.; Emsley, J. Coagulation factor XII protease domain crystal structure. *J. Thromb. Haemostasis* **2015**, *13* (4), 580−591.
(38) Daly, N. L.; Thorstholm, L.; Greenwood, K. P.; King, G. J.; Rosengren, K. J.; Heras, B.; Martin, J. L.; Craik, D. J. Structural insights into the role of the cyclic backbone in a squash trypsin inhibitor. *J. Biol. Chem.* **2013**, *288* (50), 36141−36148.
(39) Katoh, T.; Sengoku, T.; Hirata, K.; Ogata, K.; Suga, H. Ribosomal synthesis and de novo discovery of bioactive foldamer peptides containing cyclic beta-amino acids. *Nat. Chem.* **2020**, *12* (11), 1081−1088.
(40) Passioura, T.; Suga, H. A RaPID way to discover nonstandard macrocyclic peptide modulators of drug targets. *Chem. Commun.* **2017**, *53* (12), 1931−1940.
(41) Rogers, J. M.; Passioura, T.; Suga, H. Nonproteinogenic deep mutational scanning of linear and cyclic peptides. *Proc. Natl. Acad. Sci. U. S. A.* **2018**, *115* (43), 10959−10964.
(42) Baeriswyl, V.; Calzavarini, S.; Chen, S.; Zorzi, A.; Bologna, L.; Angelillo-Scherrer, A.; Heinis, C. A synthetic factor XIIa inhibitor blocks selectively intrinsic coagulation initiation. *ACS Chem. Biol.* **2015**, *10* (8), 1861−1870.
(43) Middendorp, S. J.; Wilbs, J.; Quarroz, C.; Calzavarini, S.; Angelillo-Scherrer, A.; Heinis, C. Peptide macrocycle inhibitor of coagulation factor XII with subnanomolar affinity and high target Selectivity. *J. Med. Chem.* **2017**, *60* (3), 1151−1158.
(44) Wilbs, J.; Kong, X. D.; Middendorp, S. J.; Prince, R.; Cooke, A.; Demarest, C. T.; Abdelhafez, M. M.; Roberts, K.; Umei, N.; Gonschorek, P.; Lamers, C.; Deyle, K.; Rieben, R.; Cook, K. E.; Angelillo-Scherrer, A.; Heinis, C. Cyclic peptide FXII inhibitor provides safe anticoagulation in a thrombosis model and in artificial lungs. *Nat. Commun.* **2020**, *11* (1), 3890.

https://doi.org/10.1021/jacs.1c07574
J. Am. Chem. Soc. 2021, 143, 18481−18489